EPJ Web of Conferences **140**, 03005 (2017) DOI: 10.1051/epjconf/201714003005
Powders & Grains 2017

Dry granular flows – rheological measurements of the $\mu(I)-$Rheology

Abdoulaye Fall[1*], *Michel* Badetti[1], *Guillaume* Ovarlez[2], *François* Chevoir[1] and *Jean-Noël* Roux[1]

[1]Laboratoire NAVIER, UMR 8205 CNRS-ENPC-IFSTTAR, 2 Allée Kepler 77420 Champs sur Marne, France
[2]CNRS, LOF, UMR 5258, 33600 Pessac, France

Abstract: Granular materials do not always flow homogeneously like fluids when submitted to external stress, but often form rigid regions that are separated by narrow shear bands where the material yields and flows. This shear localization impacts their apparent rheology, which makes it difficult to infer a constitutive behavior from conventional rheometric measurements. Moreover, they present a dilatant behavior, which makes their study in classical fixed-volume geometries difficult. These features led numerous groups to perform extensive studies with inclined plane flows, which were of crucial importance for the development and the validation of the μ(*I*)-rheology. Our aim is to develop a method to characterize granular materials with rheometrical tools. Using rheometry measurements in an annular shear cell, dense granular flows of 0.5mm spherical and monodisperse beads are studied. A focus is placed on the comparison between the present results and the μ(*I*)-rheology.

1 Introduction

Granular matter shows both solid and fluid behavior [1]. These materials are very sensitive to various parameters: geometry of the flow, wall roughness, flow rate, shape and size distribution of the grains, and coupling with the interstitial fluid [2]. In the dry case, the rheology is solely governed by momentum transfer and energy dissipation occurring in direct contacts between grains and with the walls. Despite the seeming simplicity of the system, the behavior of dry granular material is very rich and extends from solid to gaseous properties depending on the flow regime. In the absence of a unified framework, granular flows are generally divided into three different regimes. (i) At low shear, particles stay in contact and interact frictionally with their neighbours over long periods of time. This "quasistatic" regime of granular flow has been classically studied using modified plasticity models based on a Coulomb friction criterion [3]. The response in terms of velocity or solid fraction profiles is independent of the shear rate. (ii) Upon increasing the deformation rate, a viscouslike [4] regime occurs and the material flows more as a liquid. In this intermediate regime, the particles experience multicontact interactions. (iii) At very high velocity, a transition occurs toward a gaseous regime, in which the particles interact through binary collisions [5]. For the modeling of dense granular flows, the concept of inertial number I has been widely used and investigated with regard to its relationship with dynamic parameters, such as velocity, stress, and friction coefficient, which leads to constitutive relations for granular flows. Thus, "dynamic dilatancy" law and "friction" law were deduced from discrete simulation of two dimensional simple shear of a granular material without gravity [4]. It was observed that both dimensionless quantities: the internal friction coefficient $\mu = \tau / \sigma_N$ and the solid fraction ϕ are functions of I [4,6]. Following general results from simulations of planar shear [4] and successful applications to inclined plane flows [7], the experiments of Jop et al. [7] were carried out to quantify, for glass beads, the $\mu(I)-$rheology from the quasistatic to the rapid flow regime, corresponding to moderate I (from 0.01 to 0.5) as $\mu = \mu_s + (\mu_2 - \mu_1)/(1 + I_0 / I)$ in which μ_s, μ_2, and I_0 are three fitting parameters dependent on material properties. However, the asymptotic value of μ at high *I* was not obtained by da Cruz et al. [4] who observed an approximately linear increase of the internal friction coefficient from the static internal friction value. In 3D-simulation studies, Hatano did not either observe the asymptotic value of μ at high *I*: from $I = 10^{-4}$ to $I = 0.2$, he reported a law in which the friction coefficient increases as a power of *I* $\mu = \mu_s + \alpha I^n$ [8].

In the present work (see Fall et al. for more details [9]), we show that it is not necessary to develop specific setups (such as the inclined plane) to study dense granular flows. Indeed, we show that a simple annular shear cell can be adapted to a standard rheometer to study the rheology of granular materials under controlled confining pressure. It allows us, in particular, to obtain

* Corresponding author: abdoulaye.fall@ifsttar.fr

the dilatancy law $\phi(I)$ and also to study very accurately the quasistatic limit. Thus, from the steady state measurements of the torque and the gap during an imposed shear flow under an applied normal confining stress σ_N, we report two laws in which the internal friction coefficient and the solid fraction are functions of *I*. An effort is then made to compare the present results with the $\mu(I)-$rheology described in the literature.

2 Materials and methods

To investigate the steady flows of dry granular materials and determine the $\mu(I)-$rheology, three main features are required: (i) to avoid shear banding, (ii) to apply a confining stress in the velocity gradient direction, and (iii) to allow volume fraction variations. If one wants to use a rheometer, (i) implies that the use of a Couette cell should be avoided since it is characterized by a shear stress inhomogeneity that naturally leads to shear banding. Both the cone-and-plate and the parallel-plate geometries allow a normal force to be imposed in the velocity gradient direction; however, the analysis of the cone-and-plate flow can be performed only at a single gap value, i.e., it cannot be used to characterize a material whose the volume varies under shear. On the other hand, any gap variation in parallel-plate geometry can be accounted for in the determination of the shear rate value. Moreover, shear banding should in principle be avoided in this last geometry since the shear stress is independent of the vertical position in the gap. Nevertheless, the shear rate varies along the radial position and is equal to zero in the center. One should thus try to avoid the use of the central zone of the gap. Finally, the material should be confined by lateral walls to make sure that any gap variation actually leads to a material volume fraction variation. These requirements led us to develop a home-made annular shear cell, inspired by [10], in which pressure-imposed measurements can be performed. Annular shear cells have been extensively used to characterize the flow of pharmaceutical powders and dry granular materials [11,12]. We use a granular material made of rigid polystyrene beads (from Dynoseeds) of density $\rho_p = 1050$ kg/m^3, of diameter $d_p = 0.5$ mm (with a standard deviation of 5%). Spherical beads fill the annular box between two static concentric cylinders with, respectively, an inner and outer radii of R_i=21 mm and R_o=45 mm. The width of the annular trough is about $48d_p$ leading to a ratio of inner to outer wall radii of 0.46. We also used another annular channel with the same width but with a larger ratio of inner to outer cylinder radii equal to 0.61 (R_i=38 mm and R_o=62 mm). We have verified that changing the ratio of inner to outer cylinder radii of the annular shear cell does not significantly affect the results. The filling height (initial gap, h_0) of the annular box is adjustable from a few grain diameters (typically $5d_p$) to $30d_p$. The cylinders were finished as smoothly as possible to permit the granular material to slip there as readily as possible. For that, they are made of polyoxymethylene (POM) resin which exhibits a low friction coefficient due to the flexibility of the linear molecular chains. We have measured the friction coefficient at the wall μ_w between polystyrene beads and a plane made of POM by measuring, with our rheometer, the sliding stress under different normal stresses such as in Jenike's shear tester [13]; it is found to be very small: $\mu_w = 0.05$. The experiments were performed initially on a very dense piling $\phi_0 \approx 0.625$, close to the so called random close packing of 0.637 [14] obtained by combining a rain filling and tapping the box [15] to get a reasonably uniform packing. However, we show below that the steady state obtained when the material is sheared is the same for an initially looser piling. Granular beads are then driven by the ring-shaped upper boundary made of POM which is assembled on a *Kinexus Pro rheometer by Malvern*. To avoid wall slip, both the moving upper boundary and the static lower boundary are serrated, with 0.5mm ridges which correspond to the size of grains.

In our rheometer, instead of setting the value of the gap size for a given experiment, as in previous studies [16] and generally in rheometric measurements, we impose the normal force (i.e., the confining normal stress) and then, under shear, we let the gap size vary in order to maintain the desired value of the normal force. A typical measurement is shown in Fig. 1, where we start out with a given gap $h_0 \approx 6d_p$, impose a constant shear rate $\dot{\gamma}$ and normal force F_N and measure the torque T and the gap h as a function of strain (or time). In this case, the solid fraction ϕ is not fixed but adjusts to the imposed shear. However, it remains important to notice that, in order to keep the imposed shear rate constant, the rheometer adjusts the rotation velocity Ω since the gap varies as will be discussed below. The system reaches a steady state after a certain amount of shear strain, but we have carefully compare the transient dynamics of these quantities, beginning with freshly poured grains for two preparations, "rain piling" and "rain coupled to tapping piling" (respectively) which allow us to get the looser piling and the denser piling (respectively) samples with an initial solid fraction of 0.612 and 0.625 (respectively) [9]. As a consequence, there is no need for the sample preparation for the grains we study, namely, monodisperse spheres (note that this might not be a general result). All the annular shear cell requires is that the sample is sheared at the required normal pressure until the critical state is reached. However, it is necessary to adopt a reference packing state and ensure that the piling method used allows us to achieve sufficient repeatability for a given set materials and system parameters. Hence, we prepare all samples in the same way: a very dense material, from a rain piling coupled to tapping, is used in all the experiments presented below (the initial average volume fraction is 0.625).

3 Experimental results and analyses

We have measured the driving torque and the gap as a function of shear strain for various imposed normal force F_N (between 1 and 5N) and applied shear rate $\dot{\gamma}$ (between 0.01 and 77 s^{-1}) for a given gap $h_0 \approx 6d_p$. In Figs. 1(a-b), we show those measurements for F_N=3N and various $\dot{\gamma}$. At low shear rate, the driving torque increases slowly before reaching a steady plateau within strain of order of unity. Meanwhile, the gap fluctuates around its initial value. (We show the gap size rescaled by its initial value before shearing h/h_0 called the rescaled gap in the following.)

Upon increasing the imposed shear rate, an overshoot occurs: Its amplitude increases with increasing the shear rate. In steady state, a rate dependence of the torque is observed [Fig. 1(a)]. Moreover, increasing the imposed shear rate causes an increase of the gap size [Fig. 1(b)] allowing to quantify the dynamic dilatancy of the granular material. Notice that, with increasing the applied shear rate, large fluctuations of the driving torque and also of the gap size evolution occur in steady state flows. Similarly, in experiments in which different normal forces are imposed at a given shear rate, the steady torque is observed to increase while the steady solid fraction (steady gap) decreases when the normal force is increased. Similarly, in experiments in which different normal forces are imposed at a given shear rate [Figs. 1(c,d)], the steady torque is observed to increase while the steady solid fraction (steady gap) decreases when the normal force is increased.

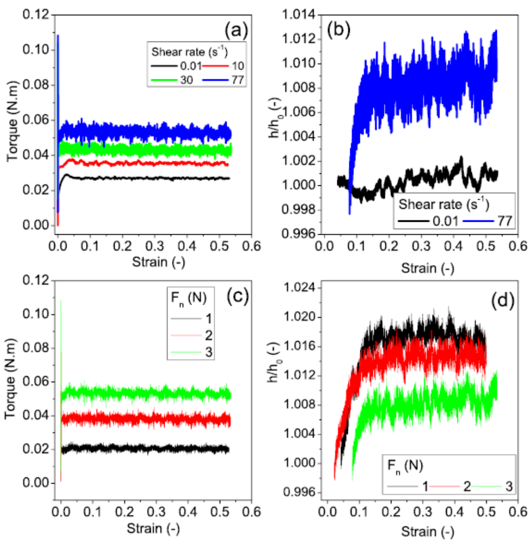

Fig. 1: Evolution as a function of the strain at 3N imposed normal force under different applied shear rates of: (a) The driving torque and (b) the rescaled gap size (only two curves are shown for clarity). Evolution as a function of the strain at 77 s-1 imposed shear rate under different applied normal forces of: (c) The driving torque and (d) the gap size rescaled by its initial value before shearing.

Once the above described experiments are combined, we can obtain the constitutive laws of the dry granular material, i.e., the dependence of the steady solid fraction ϕ and the ratio between shear and normal stresses $\mu = \tau / \sigma_N$ variation on shear rate. Indeed, from macroscopic quantities T, Ω, F_N, and h, the shear stress τ, the normal stress σ_N, shear rate $\dot{\gamma}$, and the solid fraction ϕ can be computed.

With this analysis, one can plot the shear stress in the steady state as a function of the normal stress as shown in Fig. 2(a). The first observation is that a linear relationship between the shear and normal stresses is seen for all imposed shear rates, with a slope that increases from 0.265 to 0.6 with increasing the shear rate. If an internal friction coefficient μ is defined as the ratio between shear and normal stresses, we evidence here that l is rate dependent: It increases with $\dot{\gamma}$.

The second observation is that, for all imposed shear rates, the steady value of the solid fraction decreases when one decreases the normal stress [Fig. 2(b)]. Indeed, since the grains cannot escape from the cell, one can measure unambiguously the solid fraction from the gap variation as $\phi = m / \pi\rho h(R_0^2 - R_i^2)$ in which m represents the mass of grains. Thus, $h_0 / h = \phi / \phi_0$ will simply reflect the impact of shear and confinement on dilatancy.

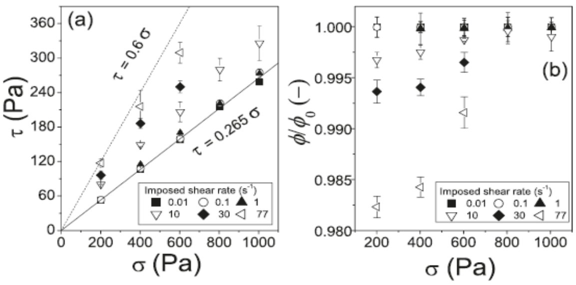

Fig. 2: Plot of the shear stress (a) and of the solid fraction rescaled by its initial value before shearing (b) as a function of the normal stress. The stress and the gap are measured in the steady state, for different imposed shear rate. The error bars come from three experiment runs.

In order to analyze the results in term of $\mu(I)$ – rheology, one has to define an inertial number such as $I = \dot{\gamma} d_p / \sqrt{\sigma_N / \rho_p}$. It varies between $10^{-7}$and 0.1 in the range of applied normal force and shear rate. This corresponds to the usual range of quasistatic to dense flow regimes. It should be noted that our annular shear geometry does not allow higher values of *I*.

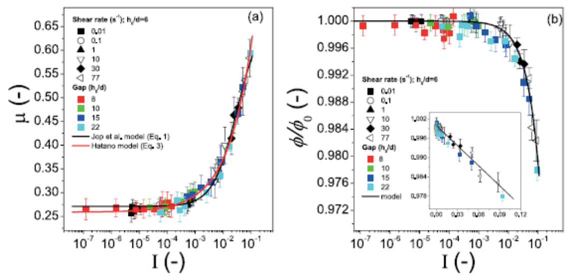

Fig. 3: Constitutive law for different sets of mean shear rates and imposed normal forces (a) friction law, i.e., effective internal friction coefficient as a function of inertial number; (b) dynamic dilatancy law, i.e., solid fraction as a function of

inertial number. The error bars come from three experiment runs.

Figure 3(a) shows how μ vary throughout the flow regimes since *I* characterizes the local rapidity of the flow. All the data obtained for different sets of shear rate and normal force collapse on a single curve τ/μ *vs. I*. For low inertial number, the internal friction coefficient tends to a finite value $\mu \approx$ 0.265 and increases with increasing *I*.

At the same time, the solid fraction variation ϕ/ϕ_0 with the inertial number *I* is shown in Fig. 3(b). Once again, all the data collapse on a single curve. At low *I*, ϕ/ϕ_0 is quasi-constant: this is the quasistatic regime. When *I* increases, the inertia starts influencing the flow and the system becomes rate dependent: the ratio ϕ/ϕ_0 decreases; this regime corresponds to the dense flow in which the granular material dilates. Moreover, in order to check the robustness of our results, we have varied the initial size of the gap. Here, with our annular shear geometry, the same experiments discussed above are made with different gap sizes from $6d_p$ to $22d_p$ and different sets of imposed shear rate and normal force. It is shown in Fig. 3 that changing the gap does not significantly affect these results. This suggests a total absence of shear localization at high inertial number. However, at small inertial number, the resolution of our measurements is not sufficient to dismiss the possibility that shear localization arises. It was indeed shown that in confined annular flow at small shear velocities and high confining pressures—small *I*—the shear may be not homogeneous and solid and fluid phases coexist [17].

4 Conclusion

From the steady state measurement of the torque and the gap, the internal friction coefficient, the solid fraction, and the inertial number *I* are measured. For low *I*, the flow goes to the quasistatic limit and the internal friction coefficient and the solid fraction profiles are independent of *I*. Upon increasing *I*, dilation occurs and the solid fraction decreases linearly when I increases while the friction coefficient increases. Comparing now these experimental results with existing models such as those of Jop et al. [7] and Hatano [8] on dry granular flows in terms of quasistatic and dense flow behaviors, our experimental data include points in range of I from 10^{-7} to 0.1 which covers quasistatic and dense flow regimes. Our measurements then show that, in this range of *I*, both models can describe our data. As a consequence, we bring evidence that rheometric measurements can be relevant to describe dry granular flows. However, additional experimental work should be carried out in order to measure the dependence of the boundary layer constitutive law on the state of the bulk material, so as to be able to describe properly the rheology when approaching the quasistatic limit.

References

1. J. Duran and R. P. Behringer, *Sands, Powders, and Grains: An Introduction to the Physics of Granular Materials* (2001).
2. B. Andreotti, Y. Forterre and O. Pouliquen, *Granular Media: Between Fluid and Solid* (2013).
3. A. Schofield and P. Wroth, Soil Use Manag. **25**, 128 (1968).
4. F. Da Cruz, S. Emam, M. Prochnow, J. N. Roux, and F. Chevoir, Phys. Rev. E - Stat. Nonlinear, Soft Matter Phys. **72**, (2005).
5. I. Goldhirsch, Annu. Rev. Fluid Mech. **35**, 267 (2003).
6. F. Chevoir, J. N. Roux, F. da Cruz, P. G. Rognon, and G. Koval, Powder Technol. **190**, 264 (2009).
7. P. Jop, Y. Forterre, and O. Pouliquen, Nature **441**, 727 (2006).
8. T. Hatano, Phys. Rev. E - Stat. Nonlinear, Soft Matter Phys. **75**, 1 (2007).
9. A. Fall, G. Ovarlez, D. Hautemayou, C. Mézière, J.-N. Roux, and F. Chevoir, J. Rheol. (N. Y. N. Y). **59**, 1065 (2015).
10. F. Boyer, É. Guazzelli, and O. Pouliquen, Phys. Rev. Lett. **107**, 1 (2011).
11. J. F. Carr and D. M. Walker, Powder Technol. **1**, 369 (1968).
12. S. B. Savage and M. Sayed, J. Fluid Mech. **53142**, 391 (1984).
13. J. Schwedes, Granul. Matter **5**, 1 (2003).
14. S. Torquato, T. M. Truskett, and P. G. Debenedetti, Phys. Rev. Lett. **84**, 2064 (2000).
15. P. Philippe and D. Bideau, Europhys. Lett. **60**, 677 (2002).
16. D. Schulze, Aufbereitungs-Technik **35**, 524 (1994).
17. Aharonov, E., and D. Sparks, Phys. Rev. E 65, 051302 (2002).